Surface-Immobilized Interpolyelectrolyte Complexes Formed by Polyelectrolyte Brushes

Artem Rumyantsev, Ekaterina Zhulina, Oleg V. Borisov

Surface-Immobilized Interpolyelectrolyte Complexes Formed by Polyelectrolyte Brushes

Journal:	*ACS Macro Letters*
Manuscript ID	mz-2023-00548x.R1
Manuscript Type:	Letter
Date Submitted by the Author:	n/a
Complete List of Authors:	Rumyantsev, Artem; University of Chicago, Chemical and Biomolecular Engineering Zhulina, Ekaterina; Institute of Macromolecular Compounds of the Russian Academy of Sciences, Borisov, Oleg; University of Pau, Laboratory of Polymer Materials

Surface-Immobilized Interpolyelectrolyte Complexes Formed by Polyelectrolyte Brushes

Artem M. Rumyantsev [1],
Ekaterina B. Zhulina[2], Oleg V. Borisov[2,3],
[1] Department of Chemical and Biomolecular Engineering,
North Carolina State University,
Raleigh, North Carolina 27695-7905, USA
[2] Institute of Macromolecular Compounds
of the Russian Academy of Sciences,
199004 St.Petersburg, Russia
[3] CNRS, Université de Pau et des Pays de l'Adour UMR 5254,
Institut des Sciences Analytiques et de Physico-Chimie
pour l'Environnement et les Matériaux, 64053 Pau, France

November 19, 2023

Abstract

A scaling theory of interaction and complex formation between planar polyelectrolyte (PE) brush and oppositely charged mobile linear PEs is developed. Counterion release is found to be the main driving force for the complexation. Interpolyelectrolyte coacervate complex (IPEC) between the brush and oppositely charged mobile PEs is formed at moderate grafting density and low salt concentration. At higher grafting density mobile chains penetrate the brush, but the brush structure is controlled by the balance between entropic elasticity and non-electrostatic short-range interactions, as it happens in a neutral brush. An increase in salt concentration beyond the theoretically predicted threshold leads to the release of the guest polyions from the brush. For brushes with moderate grafting density, complexation with oppositely charged guest polyions is predicted to trigger lateral microphase separation and formation of the finite-size surface IPEC clusters. Power-law dependencies for the cluster dimensions

on the brush grafting density, PE length, and salt concentration are provided.

email: oleg.borisov@uiv-pau.fr

For Table of Contents Use Only

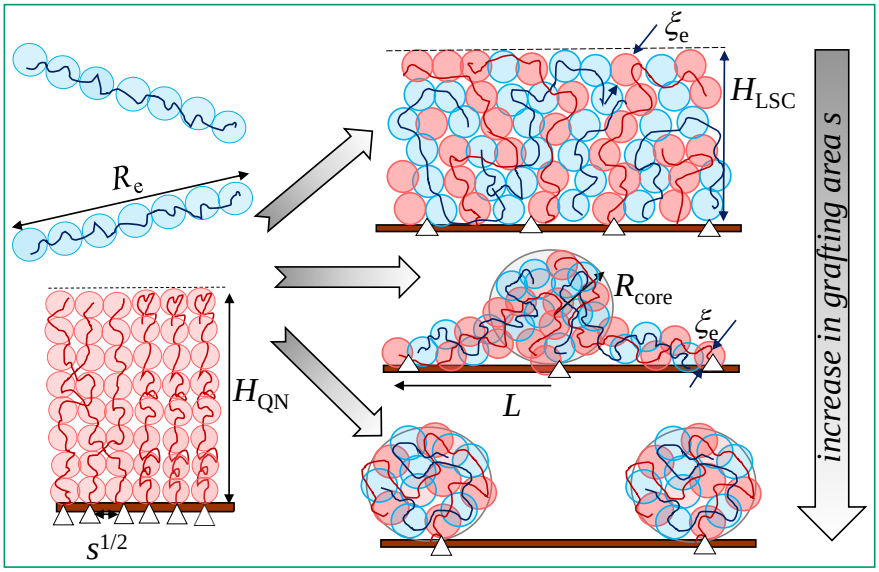

"Surface-Immobilized Interpolyelectrolyte Complexes Formed by Polyelectrolyte Brushes"

Authors: Artem M. Rumyantsev, Ekaterina B. Zhulina, Oleg V. Borisov.

Electrostatically-driven association between oppositely charged linear polyelectrolyte (PE) chains in solution[1–4] as well as aggregatively stable non-stoichiometric micellar interpolyelectrolyte complexes[5] have been extensively studied in the past few decades. In recent years, the renewed interest in interpolyelectrolyte complex (IPEC) coacervates has resulted in combined experimental, theoretical, and computational studies, which provided a deep and consistent description of the internal structure of these phases and the mechanisms underlying their formation.[6–10] These results provide a fundamental background for studying complexation in more complex systems. While important steps toward understanding scaling laws controlling micelles with complex coacervate cores[11–14] and "hybrid" coacervates formed from linear polyelectrolytes with charged nanoparticles[15,16] have already been made, complexation in polyelectrolyte brushes remains completely unexplored. The PE brushes serve as ultrathin coatings in the fabrication of smart interfaces with adhesive and tribological properties controlled by external stimuli.[17–20] We anticipate that, because of the planar geometry and lack of chains' translational mobility, the IPEComplexation in brushes should obey more complex regularities than in the bulk, and this work is aimed at deciphering them. To demonstrate this we use scaling approach well established in polymer physics.[21]

We consider a layer formed by negatively charged strong PE chains (polyanions) with the degree of polymerization N end-tethered to the planar surface and immersed into an aqueous solution. The grafting area per chain is s. The crossover between regimes of individual (non-interacting) tethered polyions and PE brush was discussed in detail in ref. 22.

The PE chains are assumed to be intrinsically flexible (the monomer unit length is on the order of Kuhn segment, a), with a fraction α of permanently negatively charged monomer units. The aqueous solution is modeled as a continuous dielectric medium with permittivity ϵ, which determines the Bjerrum length, $l_B = e^2/\epsilon k_B T$ where e is the elementary charge, k_B is Boltzmann constant and T is temperature. In the following we use reduced (dimensionless) electrostatic coupling parameter $u = l_B/a \sim 1$. We assume that water is close to Θ-solvent with respect to short-range non-electrostatic interactions between monomer units of brush-forming chains. Therefore, ternary non-electrostatic interactions, with the third virial coefficient wa^6 and $w \simeq 1$ owing to the high chain flexibility, dominate over binary excluded volume interactions inside the brush at high grafting density.

The solution contains positively and negatively charged monovalent ions of salt with concentrations (number densities) c_s and linear polycations with polymerization degree N and fraction α of positively charged monomer units. For simplicity, we assume that mobile polycations are structurally identical

to the brush-forming polyanions and water is also a Θ-solvent for them. Individual polycations in the solution as well as individual sparsely tethered to the surface (non-interacting) polyanions are stretched by intra-molecular Coulomb repulsions balanced with conformational entropic elasticity. They can be envisioned as strings of Gaussian electrostatic blobs, each of size

$$\xi_e \simeq \alpha^{-2/3} u^{-1/3}, \tag{1}$$

and their end-to-end distance are[23,24]

$$R_e \simeq N/\xi_e \simeq u^{1/3}\alpha^{2/3}N \tag{2}$$

Here and below, lengths and areas are expressed in the units of a and a^2, respectively, while salt and polymer concentrations, c_s and c_p, are given in a^{-3} units; energies and pressures are expressed in k_BT and k_BT/a^3 units, respectively.

We first review the structure of the PE brush in contact with a solution containing no oppositely charged polyions. Below we use a scaling model of the PE brush which pre-assumes (i) uniform and equal stretching of the brush-forming chains and (ii) uniform polymer concentration across the brush. This model provides (with the accuracy of numerical prefactors) experimentally accessible power law dependencies of brush thickness (and average polymer concentrations) on the brush architectural parameters s, N, α, and variable environmental conditions such as salt concentration c_s in our case.

The equilibrium structure of a polymer or PE brush is determined by the balance between repulsive inter-molecular interactions and conformational elasticity of grafted chains. In planar geometry, irrespective of the particular type of interactions, this leads to the stretching of the brush-forming chains in the direction perpendicular to the grafting surface proportional to their degree of polymerization, $H \sim N$. The latter applies also to dry or collapsed brushes. This implies that the average polymer concentration in the brush, $c \simeq N/Hs$, is independent of N.

In **Figure 1** we present the phase diagram of the PE brush in the coordinates of the area s per polyion and salt concentration c_s, which was constructed here based on results obtained in ref. 25. It contains the regimes of osmotic (O), salt-dominated (SC, SI, SR), and quasi-neutral (QN) brush, indicated by different colors, together with the expressions for boundaries. In the osmotic regime (O), the translational entropy of entrapped counterions, $F_{ions} \simeq \alpha N \ln(\alpha N/sH)$, in competition with the Gaussian elasticity of the brush-forming chains, $F_{elastic} \simeq H^2/N$ per chain, assures swelling of

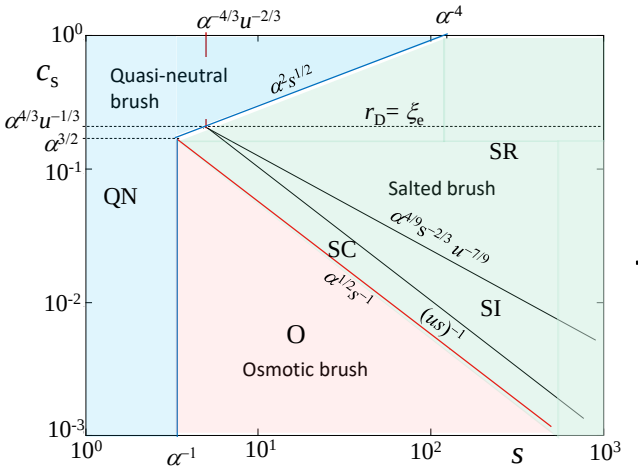

Figure 1: Diagram of states of planar PE brush in (s, c_s) log-log coordinates ($\alpha = 0.3, u = 1$). The classical picture with three regimes (osmotic O – salt-dominated classic SC – quasi-neutral QN) is retained only at $\alpha^{-1} \le s \le \alpha^{-4/3}u^{-2/3}$, and this range of s can be extended by decreasing $u \le 1$. All five regimes (O, SC, SI, SR, QN) could be attained if $\alpha^{-4/3}u^{-2/3} \le s \le \alpha^{-4}$. If $s \ge \alpha^{-4}$, then quasi-neutral regime QN is not achieved even at $c_s = 1$.

the brush up to its maximal value, $H_{OSM} \simeq \alpha^{1/2} N$. Here and below, we disregard numerical prefactors on the order of unity.

An increase in salt concentration above the threshold value $c_s \simeq \alpha^{1/2} s^{-1}$, equal to the concentration of the entrapped in the brush counterions, leads to progressive de-swelling of the brush. It happens due to the penetration of salt ions into the brush and the decrease in the differential osmotic pressure from $\Pi_{ions} \simeq \alpha c_p$ in the salt-free brush to $\Pi_{ions} \simeq \alpha^2 c_p^2 / c_s$ well above the threshold c_s value.[24,26] The balance with the elastic pressure, $\Pi_{elastic} \simeq H/Ns \simeq s^{-2} c_p^{-1}$, leads to the classical result for the thickness of salt-dominated brush, $H_{SC} \simeq \left(\alpha^2/c_s\right)^{1/3} s^{-1/3} N$.[22,27]

A more refined analysis[25] accounts for the separation of inter-chain and intra-chain electrostatic repulsions and leads to few subregimes in salt-dominated brush: (i) salt-dominated classic (SC) with exponents in thickness H_{SC} dependence coinciding with mean field exponents; (ii) SI subregime with brush thickness H_{SI} equal (in scaling terms) to the average end-to-end distance R_e of individual polyion; (iii) subregime SR with the revised exponents in H_{SR} versus salt concentration dependence, see Table 1. In all salt-dominated subregimes (SC, SI, and SR) the stretching force is governed by the differential osmotic pressure of mobile ions. In classic SC subregime, the stretching force $f_{SC} \simeq dF_{elastic}/dH \simeq H_{SC}/N$ exceeds intrinsic tension in an isolated polyion, $f_e \simeq R_e/N \simeq \xi_e^{-1}$, and $H_{SC} > R_e$. In subregime SI, the stretching force drops below f_e, and intra-molecular electrostatic repulsions keep the brush thickness $H_{SI} \simeq R_e$. In subregime SR, the Gaussian elasticity in tethered polyions is substituted by self-avoiding statistics leading to concomitant modifications in scaling exponents.[25]

As soon as the differential osmotic pressure of the mobile ions drops below that produced by non-electrostatic interactions, the brush passes into "quasi-neutral" regime (QN): Here swelling of the brush is controlled by ternary monomer-monomer repulsions with the concentration correlation length $\simeq s^{1/2}$. Notably, even in salt-free solutions, the inter-molecular non-electrostatic repulsive interactions in the brush may dominate at sufficiently high grafting density over the osmotic pressure of the counterions. As it follows from the diagram of states in Figure 1, an increase in the degree of ionization α of polyions leads to shrinkage of quasi-neutral (QN) and classic salt-dominated (SC), and expansion of osmotic (O) and other salt-dominated regimes (SI and SR).

The power law dependencies for the brush parameters in various regimes (O, SC, SI, SR, and QN) are collected in Table 1, while regimes LSC, HSC, and QN$'$ of the brush complex are discussed later.

When mobile PEs, oppositely charged with respect to the brush-forming

Table 1: Scaling laws for free PE brushes (regimes O, SC, SI, SR, and QN) and laterally uniform surface interpolyelectrolyte complexes (regimes QN′, LSC, and HSC). Table columns correspond to the normalized brush height H/N, polymer concentration c_p, and correlation length ξ in it.

Regime	H/N	$c_p = N/sH$	ξ
O (osmotic)	$\alpha^{1/2}$	$\alpha^{-1/2}s^{-1}$	$\alpha^{-1/2}$
SC (classic salt-dominated)	$(\alpha^2/c_s)^{1/3}\, s^{-1/3}$	$(\alpha^2/c_s)^{1/3}\, s^{-2/3}$	$(\alpha^2/c_s)^{-1/3}\, s^{1/3}$
SI (single polyion)	$u^{1/3}\alpha^{2/3}$	$u^{-1/3}\alpha^{-2/3}s^{-1}$	$u^{-1/3}\alpha^{-2/3}$
SR (revised salt-domianted)	$(\alpha^2/c_s)^{3/7}\, s^{-2/7}$	$(\alpha^2/c_s)^{-3/7}\, s^{-5/7}$	
QN, QN′ (quasi-neutral)	$s^{-1/2}$	$s^{-1/2}$	$s^{1/2}$
LSC (low salt coacervate)	$u^{-1/3}\alpha^{-2/3}s^{-1}$	$u^{1/3}\alpha^{2/3}$	$u^{-1/3}\alpha^{-2/3}$
HSC (high salt coacervate)	$c_s\alpha^{-2}s^{-1}$	α^2/c_s	c_s/α^2

chains, are added to the solution, they serve as multivalent counterions and may replace monovalent counterions of low molecular weight salt inside the brush, thereby neutralizing its bare charge and forming electroneutral (coacervate) complex.

The diagram of states for a planar PE brush in contact with a dilute solution of oppositely charged polyions is presented in **Figure 2**. It contains the following regimes: low salt coacervate (LSC, yellow area), high salt coacervate (HSC, green area), quasi-neutral brush with absorbed polyions (QN′, violet area), and quasi-neutral brush with expelled polyions (QN, blue area). At relatively loose grafting densities, $s > s^*$ with s^* specified later, laterally uniform coacervates decompose in clusters (white and grey areas).

Complexation is driven by the gain in translational entropy

$$\Delta F_{ions} \simeq -\alpha N \ln\left(\frac{c_{ion}}{c_s}\right) \leq 0 \tag{3}$$

due to the release of mobile counterions with concentration[24]

$$c_{ion} = c_s\left[\frac{\alpha c_p}{2c_s} + \sqrt{\left(\frac{\alpha c_p}{2c_s}\right)^2 + 1}\right]$$

from the brush to the solution. It should exceed (by the absolute value) the penalty for polyions' penetration in the brush, $\Delta F_{elastic} \simeq H_{QN}^2/N \simeq N/s$, which is caused by the increase in polymer concentration c_p and the concomitant increase in elastic stretching of the brush-forming tethered polyions. The

crossover $|\Delta F_{ions}| \simeq \Delta F_{elastic}$ can be written as

$$\left(\frac{\alpha c_p}{2c_s}\right) + \sqrt{\left(\frac{\alpha c_p}{2c_s}\right)^2 + 1} \simeq \exp\left(\frac{1}{\alpha s}\right) \tag{4}$$

with $c_p \simeq s^{-1/2}$ in quasi-neutral polymer brush. As a result, polyions remain in solution without significant brush penetration (regime QN, blue area in **Figure 2**) when the salt concentration exceeds

$$c_s^{complex} \simeq \begin{cases} \alpha s^{-1/2} \exp\left(-\alpha^{-1} s^{-1}\right), & s \leq \alpha^{-1} \\ \alpha^2 s^{1/2}, & s \geq \alpha^{-1} \end{cases} \tag{5}$$

In **Figure 2**, this threshold is indicated by the brown curve. The first line of eq. 5 was derived for $\alpha c_p \gg c_s$ and defines the boundary with regime QN′ (violet area), in which guest polyions penetrate the brush giving rise to coacervate with polymer concentration doubled as compared to that in a QN brush. Therefore the scaling dependence for the brush thickness H does not change, only the numerical prefactor increases.

The second line derived for the salt dominance case, $c_s \gg \alpha c_p$, provides the boundary between QN and HSC regimes (blue and green areas), which can be also written as $s^{1/2} \simeq \xi_{HSC}$.

Structural properties of the brush (such as its thickness H and the average polymer density in it $c_p = N/Hs$) can be found from the condition of vanishing osmotic pressure in the brush. This pressure can be presented as the sum of three contributions:

$$\Pi_{tot}(c_p) = \Pi_{elastic}(c_p) + \Pi_{vol}(c_p) + \Pi_{corr}(c_p) \tag{6}$$

The first term accounts for the conformational entropy losses in the extended brush-forming chains in the Gaussian (linear) elasticity approximation:

$$\Pi_{elastic}(c_p) \simeq -s^{-2} c_p^{-1} \tag{7}$$

The contribution of repulsive ternary monomer-monomer interactions is given by

$$\Pi_{vol}(c_p) \simeq c_p^3, \tag{8}$$

The last term Π_{corr} in eq. 6 takes into account attractions induced by the charge density correlations in coacervate, which depend on the salt concentration as follows:[28–30]

$$\Pi_{corr}(c_p) \simeq \begin{cases} -\left(\alpha^2 u c_p\right)^{3/4}, & r_D \gg \xi_e \\ -\left(\alpha^2/c_s\right)^{3/2} c_p^{3/2}, & r_D \ll \xi_e \end{cases} \tag{9}$$

In the general case, the crossover between salt-free and salt-added coacervate is given by the equality between the polymer screening radius, $r_p \simeq (\alpha^2 u c_p)^{-1/4}$, and the Debye radius due to salt, $r_D \simeq (u c_s)^{-1/2}$. For the coacervates of equilibrium densities, which are not compressed by additional (non-electrostatic) forces, the boundary $r_p \simeq r_D$ is equivalent to $r_D \simeq \xi_e$, the condition that we use in eq. 9 and which is equivalent to $c_s \simeq \alpha^{4/3} u^{-1/3}$.[31–33]

The condition of vanishing osmotic pressure, $\Pi_{tot}(c_p) = 0$, together with eqs. 6-9 defines the polymer concentration c_p within the brush and the concentration blob size. The asymptotic dependencies can be obtained for low salt concentrations ($r_D \gg \xi_e$)

$$c_p \simeq \xi^{-1} \simeq \begin{cases} \alpha^{2/3} u^{1/3}, & s \geq \alpha^{-4/3} u^{-2/3}, \text{ LSC regime} \\ s^{-1/2}, & s \leq \alpha^{-4/3} u^{-2/3}, \text{ QN}' \text{ regime} \end{cases} \quad (10)$$

and high salt concentrations ($r_D \ll \xi_e$)

$$c_p \simeq \xi^{-1} \simeq \begin{cases} \alpha^2 / c_s, & s \geq \alpha^{-4} c_s^2, \text{ HSC regime} \\ s^{-1/2}, & s \leq \alpha^{-4} c_s^2, \text{ QN regime} \end{cases} \quad (11)$$

In eqs. 10 and 11, the first lines correspond to the equilibrium density of the coacervate, which is controlled by the balance between correlation attractions and ternary repulsion, i.e., the second and the third terms in eq. 6; remarkably, in these regimes, the average polymer concentration in the brush is approximately independent of grafting density, $1/s$, but the chains in the brush remain stretched with respect to their Gaussian dimensions, $H \gg N^{1/2}$. The second lines describe the brush in a quasi-neutral regime, when equilibrium chain stretching and hence the average polymer concentration in the brush is controlled by the balance of conformational entropy and three-body repulsions, the first and the second terms in eq. 6.

For low salt regimes described by eq. 10, the boundary between the unperturbed coacervate layer (the first line) and quasi-neutral brush (the second line) can be also written as $s \simeq \xi_e^2$. At high salt concentrations, eq. 11, the analogous crossover is $s \simeq \xi_{HSC}^2$, with $\xi_{HSC} \simeq \alpha^{-2} c_s$ equal to the correlation length in the salt-added coacervate.[30–33]

To recapitulate, complexation results in the brush collapse in LSC and HSC regimes but, in contrast, leads to increasing the brush thickness in regime QN′.

Our findings are rigorous when correlations between polymer charges are weak, i.e., each electrostatic blob (in SI and LSC regimes) contains many charges, $u\alpha^{1/2} \leq 1$.[31,33] This ensures $c_p \ll 1$ in IPEC and enables neglecting polymer-solvent dielectric mismatch. We expect quantitative agreement

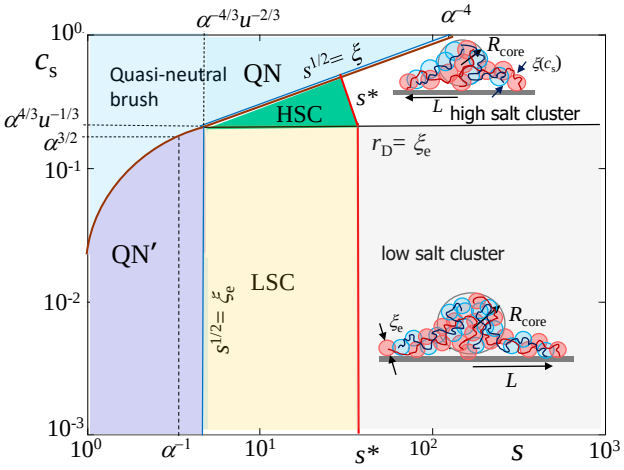

Figure 2: Diagram of states of planar PE brush with added oppositely charged polyions in s vs c_s log-log coordinates ($\alpha = 0.3, u = 1, N = 500$). The Brown line given by eq. 5 shows the boundary of complexation in the brush. Above this line, polyions do not penetrate the brush. Below this line, polyions penetrate quasi-neutral brush to substitute counterions and form laterally uniform coacervates (violet, yellow, and green areas) and clusters that are either "salt-free" (grey area) or salt-dominated (white area). Individual globules with $p = 1$ are predicted at larger $s^{**} \geq 10^3$ (not shown). Decomposition of laterally uniform coacervates in clusters stars to the right of red lines indicating s^*. Because $H_{QN} \geq R_{core}$ at the boundary QN–high salt cluster, the decomposition of QN brush into clusters is accompanied by a jumpwise decrease in the brush thickness.

in exponents for weakly charged PEs[10] with $\alpha < 1$ and (at least) semi-quantitative validity for chains with $\alpha \approx 1$. Similarly, salt concentration should obey $c_s \leq u^{-3}$. These constraints are assumed fulfilled throughout the entire paper.

At relatively loose grafting of polyions, the formation of IPEC between the grafted chains and guest oppositely charged PEs may trigger lateral instability in the PE brush. It results in the formation of pinned clusters, each with the globular IPEC core comprising fragments of several chains, which are connected by stretched segments (strings) to the grafting points (depicted by insets in **Figure 2**). The onset of the decomposition of the laterally uniform brush into clusters with finite aggregation numbers coincides with a loss of stretching of the brush-forming chains, $H_{LSC} \simeq N^{1/2}$ and $H_{HSC} \simeq N^{1/2}$ (red lines in **Figure 2**).

The equilibrium aggregation number (number of tethered chains in one cluster) p can be found from the condition of a minimum of the free energy per chain in a cluster

$$\frac{\Delta F_{cluster}(p)}{p} = \frac{F_{cluster}(p)}{p} - F(p=1) \tag{12}$$

where

$$F_{cluster}(p) = \mu p N + \gamma A_{cluster}(p) + p F_{string}(p) \tag{13}$$

and $F(p=1) = N\mu + \gamma A(p=1)$ is the reference free energy of an IPEC formed by a single tethered PE chain ($p=1$) with an oppositely charged PE; $\mu < 0$ is the chemical potential of a monomer unit in IPEC, $\gamma \simeq \xi^{-2}$ is the surface tension at the IPEC/water interface,[31] and $A(p \geq 1) \simeq (pN/c_p)^{2/3} = p^{2/3} A(p=1)$ is the interfacial area of the cluster comprising p brush chains and p guest PEs. The free energy of a pinned cluster with $p \geq 1$ chains additionally includes the contribution of p stretched strings connecting the cluster core to p grafting points of the chains forming the cluster.

In calculating F_{string}, we assume that each string has the structure of a neutral "zipper" with the guest PE chain segment locally bound to the tethered PE (linear IPEC). The balance between the elastic and the surface energy of the string results in the string thickness of the order of the blob size within the globular part of the complex, ξ. The in-plane dimension of the cluster is $L \simeq (ps)^{1/2}$, and the string free energy is equal to the number of blobs in it:

$$F_{string} \simeq \gamma L \xi \simeq \frac{L}{\xi} \simeq (ps)^{1/2} \xi^{-1} \tag{14}$$

This result is well-known in the context of string-globule coexistence in single polymer chains,[34,35] and the standard relationship between the number of

monomers in the blob g and the surface tension γ counted in units of k_BT/a^2 has been employed:

$$|\mu| \simeq \gamma \simeq g^{-1} \simeq \xi^{-2} \tag{15}$$

The minimization of the free energy per chain given by $\frac{\partial}{\partial p}\frac{\Delta F_{cluster}(p)}{p} = 0$ provides power law expressions for the cluster properties

$$p \simeq \xi^{-2/5} s^{-3/5} N^{4/5} \tag{16}$$

$$L \simeq (ps)^{1/2} \simeq \xi^{-1/5} s^{1/5} N^{2/5} \tag{17}$$

$$R_{core} \simeq \left(\frac{pN}{c_p}\right)^{1/3} \simeq \xi^{1/5} s^{-1/5} N^{3/5} \tag{18}$$

where R_{core} is the size of the cluster's core and $c_p \simeq g/\xi^3 \simeq \xi^{-1}$ has been used to arrive at the last representation.

As follows from the equations, upon an increase in the grafting density s^{-1}, the size L of the lateral footprint of the cluster decreases whereas the core size R_{core} increases. The onset of the laterally uniform brush's decomposition into the clusters can be found from $L \simeq R_{core}$ and reads

$$s^* \simeq \xi N^{1/2} \tag{19}$$

At very low grafting density clusters split into globular IPECs formed by individual chains, $p = 1$, the characteristic threshold in terms of grafting density is given by

$$s^{**} \simeq \xi^{-2/3} N^{4/3} \tag{20}$$

By substituting the correlation lengths $\xi_{LSC} \simeq u^{-1/3}\alpha^{-2/3}$ and $\xi_{HSC} \simeq c_s/\alpha^2$ for LSC and HSC regimes into eqs. 16-20, one finds the parameters of clusters

$$p \simeq N^{4/5} s^{-3/5} \begin{cases} \left(\alpha^{2/3} u^{1/3}\right)^{2/5} & \text{low salt cluster} \\ \left(\alpha^2/c_s\right)^{2/5} & \text{high salt cluster} \end{cases} \tag{21}$$

$$L \simeq (ps)^{1/2} \simeq N^{2/5} s^{1/5} \begin{cases} \left(\alpha^{2/3} u^{1/3}\right)^{1/5} & \text{low salt cluster} \\ \left(\alpha^2/c_s\right)^{1/5} & \text{high salt cluster} \end{cases} \tag{22}$$

$$R_{core} \simeq N^{3/5} s^{-1/5} \begin{cases} \left(\alpha^{2/3} u^{1/3}\right)^{-1/5} & \text{low salt cluster} \\ \left(\alpha^2/c_s\right)^{-1/5} & \text{high salt cluster} \end{cases} \tag{23}$$

and the ranges of their thermodynamic stability

$$s^* \simeq N^{1/2} \begin{cases} \alpha^{2/3} u^{1/3} & \text{low salt} \\ \alpha^2 c_s^{-1} & \text{high salt} \end{cases} \tag{24}$$

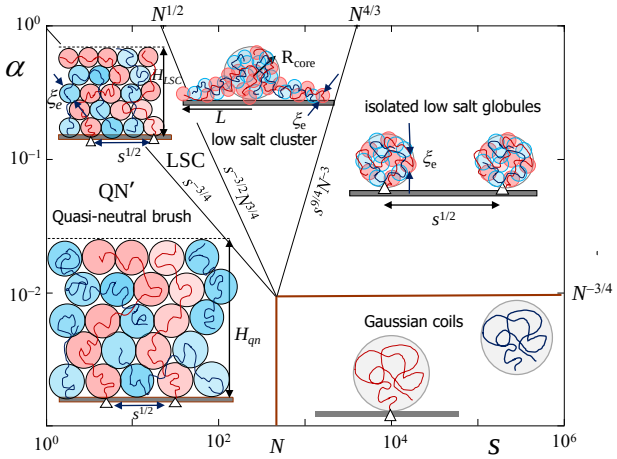

Figure 3: Diagram of states of planar salt-free PE brush in contact with a dilute solution of oppositely charged polyions in α, s log-log coordinates ($N = 500, u = 1$). Insets demonstrate blob structure in regimes of quasi-neutral brush (QN′), low salt coacervate (LSC), low salt cluster, isolated globules, and Gausian coils. Black boundaries separate brush regimes with penetrated polyions. In the regime of Gaussian coils (with brown boundaries) mobile polyions do not form complexes with oppositely charged tethered chains.

$$s^{**} \simeq N^{4/3} \begin{cases} \alpha^{4/9} u^{2/9} & \text{low salt} \\ \alpha^{4/3} {c_s}^{-2/3} & \text{high salt} \end{cases} \tag{25}$$

under low and high salt conditions, respectively.

Notably, equations 16-20 with ξ representing the thermal blob size, are also applicable to neutral polymer brushes in a poor solvent, which were shown to exhibit similar lateral microphase separation.[36–38]

In **Figure 3** we present the diagram of states of PE brush in contact with the solution of oppositely charged polyions in log-log coordinates of α and s under low salt conditions. It comprises IPEC regimes QN′, LSC, low salt cluster, and individual globules, which are separated by black boundaries. In the regime of Gaussian coils (with orange boundaries), mobile polyions stay separated from tethered ones. Insets illustrate blob structure in all the

regimes, with the boundaries between regimes indicated.

To, conclude, in this work, we have considered complex coacervation between polyanionic brush and mobile polycations. The conditions necessary for the formation of the surface-immobilized IPEComplex have been established, and the internal structure of the resulting surface-immobilized IPEC layer has been described.

When salt concentration is low, the entropy gain due to counterion release and replacement by mobile polycations is high and laterally uniform complex formation takes place if the brush is initially in osmotic or quasi-neutral regime. Interestingly, the driving force for IPEC formation with brushes is different from macroscopic complexation, in which the entropy gain[39,40] should be primarily associated not with counterions but rather with the orientational degrees of freedom of the solvent molecules.[9] As it is anticipated in refs. 41-42, the counterion release provides also the major driving force for the uptake of globular proteins by PE brushes. At sufficiently high grafting density the structure of the brush IPEC is controlled by a balance of the ternary repulsions and conformational elasticity, like in the quasi-neutral brush, while correlational attraction provides a relatively small contribution to the free energy balance. The penetration of the guest polyions and IPEComplexation in the brush is suppressed at high salt concentrations when counterion release provides a much lower entropy gain compared to enhanced ternary repulsions so that the brush free of guest chains is found in a quasi-neutral regime.

Similarly to non-ionic polymer brushes in a poor solvent, initially uniform osmotic PE brushes may exhibit complexation-induced lateral instability and split into finite-size clusters with IPEC cores, which are connected by stretched strings to multiple grafting points. We believe that the theory of IPEComplexation in brushes developed herein will stimulate experimental and simulation activity in this area.

Acknowledgments

This work was supported by Russian Science Foundation, grant 23-13-00174

References

[1] Kabanov, V.A. In: Dubin, P.; Bock, J.; Davies, R.M.; Schulz, D.N. Thies, C. Editors, *Macromolecular complexes in chemistry and biology* Berlin: Springer, 1994, p. 151–174.

[2] Philipp, B.; Dautzenberg, H.; Linow, J.K.; Dawydoff, W. Polyelectrolyte complexes — Recent developments and open problems. *Prog. Polym. Sci.* **1989**, *14*, 91–172.

[3] Kabanov, A.V.; Kabanov, V.A. Interpolyelectrolyte and block ionomer complexes for gene delivery: Physico-chemical aspects. *Adv. Drug Deliv. Rev.* **1998**, *30*, 49–60.

[4] Gucht, J. van der; Spruijt, E.; Lemmers, M.; Cohen Stuart, M. A. Polyelectrolyte complexes: bulk phases and colloidal systems. *J. Colloid Interface Sci.* **2011**, *361*, 407–422.

[5] Pergushov, D.V.; Müller, A.H.E.; Schacher, F.H. Micellar interpolyelectrolyte Complexes. *Chem. Soc. Revs.* **2012**, *41*, 6888–6901

[6] Srivastava, S.; Tirrell, M. V. Polyelectrolyte complexation. *Adv. Chem. Phys.* **2016**, *161*, 499–544.

[7] Rumyantsev, A. M.; Jackson, N. E.; de Pablo, J. J. Polyelectrolyte complex coacervates: Recent developments and new frontiers. *Annu. Rev. Condens. Matter Phys.* **2021**, *12*, 155–176.

[8] Sing, C. E.; Perry, S. L. Recent progress in the science of complex coacervation. *Soft Matter* **2020**, *16*, 2885–2914.

[9] Chen, S.; Wang, Z.-G. Driving force and pathway in polyelectrolyte complex coacervation. *Proc. Natl. Acad. Sci. U.S.A.* **2022**, *119*, e2209975119.

[10] Fang, Y. N.; Rumyantsev, A. M.; Neitzel, A. E.; Liang, H.; Heller, W. T.; Nealey, P. F.; Tirrell, M. V.; de Pablo, J. J. Scattering evidence of positional charge correlations in polyelectrolyte complexes. *Proc. Natl. Acad. Sci. U.S.A.* **2023**, *120*, e2302151120.

[11] Rumyantsev, A. M.; Zhulina, E. B.; Borisov, O. V. Scaling theory of complex coacervate core micelles. *ACS Macro Letters* **2018**, *7*, 811–816.

[12] Marras, A. E.; Campagna, T. R.; Vieregg, J. R.; Tirrell, M. V. Physical property scaling relationships for polyelectrolyte complex micelles. *Macromolecules* **2021**, *54*, 6585–6594.

[13] Marras, A. E.; Ting, J. M.; Stevens, K. C.; Tirrell, M. V. Advances in the structural design of polyelectrolyte complex micelles. *J. Phys. Chem. B* **2021**, *125*, 7076–7089.

[14] Stevens, K. C.; Marras, A. E.; Campagna, T. R.; Ting, J. M.; Tirrell, M. V. Effect of charged block length mismatch on double diblock polyelectrolyte complex micelle cores. *Macromolecules* **2023**, *56*, 5557–5566.

[15] Rumyantsev, A. M.; Borisov, O. V.; de Pablo, J. J. Structure and dynamics of hybrid colloid–polyelectrolyte coacervates. *Macromolecules* **2023**, *56*, 1713–1730.

[16] Yu, B.; Liang, H.; Nealey, P. F.; Tirrell, M. V.; Rumyantsev, A. M.; de Pablo, J. J. Structure and dynamics of hybrid colloid–polyelectrolyte coacervates: Insights from molecular simulations. *Macromolecules* **2023**, *56*, 7256–7270.

[17] Birshtein, T. M., Amoskov, V. A. Polymer brushes. *Polymer Science, Ser. C* **2000**, *42*, 172–207.

[18] Ballauff, M.; Borisov, O. V. Polyelectrolyte brushes. *Curr. Opin. Colloid Interface Sci.* **2006**, *11*, 316–323.

[19] Minko, S. *Responsive Polymer Materials: Design and Applications*; Blackwell Publishing Ltd.: Oxford, 2006

[20] Rühe, J.; Ballauff, M.; Biesalski, M.; Dziezok, P.; Gröhn, F.; Johannsmann, D.; Houbenov, N.; Hugenberg, N.; Konradi, R.; Minko, S.; Motornov, M.; Netz, R. R.; Schmidt, M.; Seidel, C.; Stamm, M.; Stephan, T.; Usov, D.; Zhan, H. Polyelectrolyte brushes. *Adv. Polym. Sci.* **2004**, *165*, 79–150.

[21] de Gennes, P.-G. *Scaling Concepts in Polymer Physics*; Cornell University Press: Ithaca and London, 1979

[22] Borisov, O. V.; Zhulina, E. B.; Birshtein, T. M. Diagram of the states of a grafted polyelectrolyte layer. *Macromolecules* **1994**, *27*, 4795–4803.

[23] de Gennes, P.-G. d; Pincus, P.; Velasco, R. M.; Brochard, F. Remarks on polyelectrolyte conformation. *J. Phys. (Paris)* **1976**, *37*, 1461–1473.

[24] Dobrynin, A. V.; Rubinstein, M. Theory of polyelectrolytes in solutions and at surfaces. *Prog. Polym. Sci.* **2005**, *30*, 1049–1118.

[25] Zhulina, E. B.; Rubinstein, M. Ionic strength dependence of polyelectrolyte brush thickness. *Soft Matter* **2012**, *8*, 9376–9383.

[26] Oosawa F. *Polyelectrolytes;* New York: Marcel Dekker; 1971.

[27] Pincus, P.A. Colloid stabilization with grafted polyelectrolytes. *Macromolecules* **1991**, *24*, 2912–2919;

[28] Borue, V. Yu.; Erukhimovich, I. Ya. A statistical theory of weakly charged polyelectrolytes: Fluctuations, equation of state and microphase separation. *Macromolecules* **1988**, *21*, 3240–3249.

[29] Borue, V. Y.; Erukhimovich, I. Y. A statistical theory of globular polyelectrolyte complexes. *Macromolecules* **1990**, *23*, 3625–3632.

[30] Castelnovo, M.; Joanny, J.-F. Formation of polyelectrolyte multilayers. *Langmuir* **2000**, *16*, 7524–7532.

[31] Rumyantsev, A. M.; Zhulina, E. B.; Borisov, O. V. Complex coacervate of weakly charged polyelectrolytes: Diagram of states. *Macromolecules* **2018**, *51*, 3788–3801.

[32] Rubinstein, M.; Liao, Q.; Panyukov, S. Structure of liquid coacervates formed by oppositely charged polyelectrolytes. *Macromolecules* **2018**, *51*, 9572–9588.

[33] Danielsen, S. P. O.; Panyukov, S.; Rubinstein, M. Ion pairing and the structure of gel coacervates. *Macromolecules* **2020**, *53*, 9420–9442.

[34] Halperin, A.; Zhulina, E. B. On the deformation behaviour of collapsed polymers. *Europhys. Lett.* **1991**, *15*, 417–421.

[35] Dobrynin, A. V.; Rubinstein, M.; Obukhov, S. P. Cascade of transitions of polyelectrolytes in poor solvents. *Macromolecules* **1996**, *29*, 2974–2979.

[36] D.R.M. Williams. Grafted polymers in bad solvents: octopus surface micelles. *Journal de Physique II* **1993**, *3*, 1313–1318.

[37] Zhulina, E.B.; Birshtein, T.M.; Priamitsyn, V.A.; Klushin, L.I. Inhomogeneous structure of collapsed polymer brushes under deformation. *Macromolecules* **1995**, *28*, 8612–8620.

[38] Soga, K. G.; Guo, H.; Zuckermann, M. J. Polymer brushes in a poor solvent. *Europhys. Lett.* **1995**, *29*, 531–536.

[39] Priftis, D.; Laugel, N.; Tirrell, M. Thermodynamic characterization of polypeptide complex coacervation. *Langmuir* **2012**, *28*, 15947–15957.

[40] Chang, L.-W.; Lytle, T. K.; Radhakrishna, M.; Madinya, J. J.; Velez, J.; Sing, C. E.; Perry, S. L. Sequence and entropy-based control of complex coacervates. *Nature Commun.* **2017**, *8*, 1273.

[41] Wittemann, A.; Haupt, B.; Ballauff, M. Adsorption of proteins on spherical polyelectrolyte brushes in aqueous solution. *Phys.Chem.Chem.Phys.* **2003**, *5*, 1671–1677.

[42] Achazi, K.; Haag, R.; Ballauff, M.; Dernedde, J.; Kizhakkedathu, J.N.; Maysinger, D.; Multhaup, G. Understanding the interactions of polyelectrolyte architectures with proteins and biosystems. *Angewandte Chemie Int. Ed.* **2021**, *60*, 3882–3904.